Iran J Sci Technol Trans Mech Eng (2019) 43:663–673
https://doi.org/10.1007/s40997-018-0231-4

RESEARCH PAPER

Comparison of Numerical Methods for Two-Fluid Model for Gas–Liquid Transient Flow Regime and Its Application in Slug Modeling Initiation

H. Zolfaghary Azizi[1] · M. Naghashzadegan[1] · V. Shokri[2]

Received: 28 February 2017 / Accepted: 14 July 2018 / Published online: 17 August 2018

Abstract
The formation of slug in the horizontal pipes due to the hydrodynamic instabilities has always been of great interest to many researchers. In this research, the effect of various numerical methods on the simulation of slug flow initiation using pressure-free two-fluid model has been investigated. The two-fluid model has been solved by conservative shock-capturing method. When the slug is formed, a strong discontinuity will be developed in the flow stream. Therefore, a numerical method should have the capability to predict this discontinuity with high accuracy and should not have oscillation near the discontinuity. There are three different models to simulate two-phase flow systems: homogeneous equilibrium model, drift-flux model, and two-fluid model. This research used two-fluid model for predicting the slug flow initiation through a pipe. Four different numerical two-fluid methods, namely Lax-Friedrichs, Rusanov, Richtmyer and flux-corrected transport (FCT) have been used in this research. Results show that FCT is the most accurate method for the prediction of the slug flow initiation among other methods where Rusanov and Lax-Friedrichs numerical methods were in the next steps, respectively. Due to the oscillatory nature near the discontinuity caused by formation of slug regime, the Richtmyer numerical method is not an appropriate method for modeling slug flow regime. Results also show that as the numerical diffusion of these methods reduces in the flow field, the slug flow initiation will be predicted with higher accuracy.

Keywords Slug flow · Two-fluid model · Two-phase transient flow · Numerical simulation

1 Introduction

Accurate prediction of fluid dynamics associated with two-phase flow has always been of utmost importance, for example, in the oil industry, through the transportation of crude oil from offshore rigs to the beach equipment such as cleaners and separators, where there might be a possible mixture of crude oil, gas, water and dispersed sand particles. Besides, there is also a two-phase flow of steam and water flowing inside the pipes in the steam power plants and cooling nuclear power plants. In general, there are three different models to simulate two-phase flow systems: homogeneous equilibrium model (Omgba-Essama 2004), drift-flux model (Ishii 1975) and two-fluid model (Ishii 1975; Ishii and Mishima 1984). This research focuses on the two-fluid model. In the two-fluid model formulation, the conservation equations (mass, momentum and energy) have been considered for each phase separately. More precise details of each phase are provided by this model, and this model is the best model among the two-phase flow models (Issa and Kempf 2003). Averaged form of the two-fluid model is based on surface averaging of the three-dimensional equations so that all the flow quantities on the pipe surface are integrated and subsequently are replaced using appropriate average (Wallis 1969). Interactions between the liquid and gas phases are presented by closure relations that have a significant effect on the flow field. For slug flow modeling, a model that can have the ability to predict the transition from the stratified regime to wave and then to slug is the slug capturing model (Issa and Kempf 2003).

The method described in the current paper is a slug capturing technique in which the slug flow regime is

✉ M. Naghashzadegan
naghash2001@yahoo.com

[1] Department of Mechanical Engineering, University of Guilan, P.O. Box 3756, Rasht, Iran

[2] Department of Mechanical Engineering, Sari Branch, Islamic Azad University, Sari, Iran

predicted as a mechanistic and automatic outcome of the growth of hydrodynamic instabilities (Woodburn and Issa 1998).

Issa and Kempf (2003) simulated the slug flow in horizontal and inclined pipes using slug capturing model. However, the two-fluid model was in ill-posed condition and their outputs were limited to the flow conditions under which the roots of the characteristic equation were real. While the two-fluid model is mathematically well posed, the growing instability of the stratified flow leading to slug flow is obtained.

Bonizzi and Issa (2003a) modeled the gas bubbles entrainment into the slug body and improved the closure relations for modeling of the bubble entrainment into the liquid slug body and interfacial shear stresses. Later on (2003), they studied the three-phase slug modeling (Bonizzi and Issa 2003b).

Omgba-Essama (2004) solved two-fluid four equations using central numerical methods. They evaluated the slug growth and development by employing these methods and used an adaptive network to improve the efficiency of the methods.

Carneiro et al. (2005) and Hanyang and Ligjin (2005) investigated the interfacial instabilities and slug initiation regime in the gas–liquid flow in horizontal pipes using transient two-fluid model.

Ujang et al (2006) experimentally studied the effects of pressure and superficial velocity of gas and liquid on the slug flow initiation as well as on the hydrodynamic slugs formed in the downstream of the pipe. They concluded that the maximum number of slugs occurs in the first 3 m of the pipe. Also, the frequency of slug formation is a weak function of pressure. Although the higher pressure delays the slug flow initiation.

Issa et al. (2006) presented a more detailed closure model for the simulation of bubble entrainment into the liquid slug body and interfacial shear stresses. Closure models are important because specific equations have not been provided for them yet (Issa et al. 2006).

Wang et al. (2007) reported that due to the limitations of the operational space, the experimental slug flow studies are performed in short pipes and in the low rate flows of gas and liquid. They investigated the slug flow initiation in the two-phase gas–liquid flow in a horizontal pipe with the diameter of 0.095 m. They concluded that the formation of slug depends on the superficial velocity of gas as well as the local height of liquid in the channel.

Ansari and Shokri (2011) presented a technique for the prediction of the initiation and growth of liquid clots in the horizontal container. They solved the governing equations of the transient compressible two-fluid model, using groups of high-resolution shock-capturing methods. They considered the direct calculation of clot formation and growth in the stratified flow by solving flow field equations. In addition, since high-order methods do not have dispersion properties, precise modeling of the existing discontinuity in the flow field due to the presence of clots has been done with high accuracy (Ansari and Shokri 2011).

Issa et al. (2011) carried out the accurate simulation of the continuous slug flow using two-fluid model in oil and gas pipelines. They assumed a hydrostatic pressure for gas and liquid phases in their model (Issa et al. 2011).

Cazarez-Candia et al. (2011) simulated the isotherm slug flow without phase change via two-fluid model using single-cell model with finite-difference numerical method.

Simoes et al. (2014) simulated the prediction of slug frequency without mass transfer in a horizontal pipe using two-fluid model via a finite-volume numerical method.

Zeng et al. (2015), using two-fluid model, performed comparison of implicit and explicit AUSM-family numerical schemes for compressible multi-phase flows.

Bonzanini et al. (2017) proposed a numerical resolution of a one-dimensional (1D), transient, simplified two-fluid model regularized with an artificial diffusion term for modeling stratified, wavy and slug flow in horizontal and nearly horizontal pipes. They concluded that the artificial diffusion can prevent the unbounded growth of instabilities where the one-dimensional two-fluid model is ill-posed (Bonzanini et al. 2017).

Shokri and Esmaeili (2017) presented a numerical study using the two-fluid model in order to compare the effect of hydrodynamic and hydrostatic models for pressure correction term in the two-fluid model in gas–liquid two-phase flow modeling to provide a more accurate model. They concluded that the hydrodynamic pressure correction term in two-fluid equations system is hyperbolic in a broader range than hydrostatic pressure correction term.

This study is about the modeling of the two-phase slug flow initiation and based on the numerical solution of the transient two-fluid model equations. The advantage of this method is that the flow field is allowed to develop naturally from initial conditions and the slug evolves automatically as a product of the computed flow. The need for the many empirical models for flow regime transition can thus be minimized. As a consequence of the literature survey, the capability of the numerical methods for the prediction of the slug flow initiation has not been investigated so far. In the present research, using the *Riemann* solver, it is aimed to show the capability of the numerical methods to predict the isothermal slug flow initiation and its growth via the two-fluid model.

2 The Two-Fluid Model

2.1 Governing Equations

The two-fluid model consists of two conservation equations of mass, momentum and energy for each phase. One-dimensional form of this model is obtained from the surface integration of flow properties on a cross section of the stream (Ishii 1975). The momentum transfer between each phase and wall and also the dynamic interaction between phases at the interface appear as source terms in the model, for which the empirical formula should be applied for calculation (Ishii and Mishima 1984). In the present study, the flow has been assumed as isotherm. One-dimensional equations for two-fluid model are obtained as follows.

Gas mass conservation equation:

$$\frac{\partial}{\partial t}(\rho_G A_G) + \frac{\partial}{\partial x}(\rho_G A_G V_G) = 0 \tag{1}$$

Liquid mass conservation equation:

$$\frac{\partial}{\partial t}(\rho_L A_L) + \frac{\partial}{\partial x}(\rho_L A_L V_L) = 0 \tag{2}$$

Gas momentum conservation equation:

$$\begin{aligned}\frac{\partial}{\partial t}(\rho_G A_G V_G) + \frac{\partial}{\partial x}\left(\rho_G A_G V_G^2\right) = &- A_G \frac{\partial P_I}{\partial x} \\ &- A_G \rho_G g \cos\beta \frac{\partial h_L}{\partial x} \\ &- A_G \rho_G g \sin\beta - \tau_G S_G \\ &- \tau_I S_I\end{aligned} \tag{3}$$

Liquid momentum conservation equation:

$$\begin{aligned}\frac{\partial}{\partial t}(\rho_L A_L V_L) + \frac{\partial}{\partial x}\left(\rho_L A_L V_L^2\right) = &- A_L \frac{\partial P_I}{\partial x} \\ &- A_L \rho_L g \cos\beta \frac{\partial h_L}{\partial x} \\ &- A_L \rho_L g \sin\beta - \tau_L S_L \\ &+ \tau_I S_I\end{aligned} \tag{4}$$

In the above equations for kth phase ($k = G$ is the gas phase and $k = L$ is the liquid phase), ρ_k is the density of kth phase, V_k is the velocity of kth phase, A_k is the flow cross section of kth phase, P_I is the interface pressure. g is the acceleration of gravity, β is pipe inclination angle, h_L height of the liquid level from the bottom of the pipe and τ_G, τ_L and τ_I represent gas wall shear stress, liquid wall shear stress and interface shear stress, respectively. S_G, S_L and S_I also represent the wet gas environment, liquid and interface, respectively.

The two-fluid model that includes Eqs. (1)–(4) is called single-pressure four-equation model. In many numerical methods which are used to solve hyperbolic equations, the given equations should be written in conservative form. Watson (1990) has done this as follows.

Total mass conservation equation is obtained from the summation of Eqs. (1) and (2).

Mass conservation equation:

$$\frac{\partial}{\partial t}(\rho_L A_L + \rho_G A_G) + \frac{\partial}{\partial x}(\rho_L A_L V_L + \rho_G A_G V_G) = 0 \tag{5}$$

The momentum conservation equation is obtained from the combination of Eqs. (3) and (4) and eliminating interface pressure, P_I, from two equations. The interface pressure P_I is never employed while utilizing this model. During the liquid height changes, P_I is derived from the overall momentum equation robustly.

Momentum conservation equation:

$$\begin{aligned}&\frac{\partial}{\partial t}(\rho_L V_L + \rho_G V_G) \\ &\quad + \frac{\partial}{\partial x}\left(\frac{1}{2}\rho_L V_L^2 - \frac{1}{2}\rho_G V_G^2 + (\rho_L - \rho_G) g \cos\beta h_L\right) = H\end{aligned} \tag{6-a}$$

$$H = -(\rho_L - \rho_G) g \sin\beta + \left(\frac{1}{A_L} + \frac{1}{A_G}\right)\tau_I S_I + \frac{\tau_G S_G}{A_G} - \frac{\tau_L S_L}{A_L} \tag{6-b}$$

Variables in this system of equations are A_G, A_L, V_G and V_L terms, where only two equations are available for this system. Therefore, two other equations are needed. The first equation is the geometric restriction for two phases that can be expressed as follows:

$$A_L + A_G = A, \tag{7}$$

where A is the total pipe cross-sectional area. The second equation can be obtained from mass Eqs. (1) and (2). If the two phases are incompressible, we can write:

$$\frac{\partial}{\partial x}(A_L V_L + A_G V_G) = 0 \tag{8-a}$$

The terms $A_L V_L + A_G V_G$ are independent of the pipe axis. It can be written as a function of time as $C(t)$, which is a known function but is dependent on the flow at the inlet boundary condition:

$$A_L V_L + A_G V_G = C(t) = (A_L V_L + A_G V_G)_{\text{inlet}} \tag{8-b}$$

Inlet means the condition at the entrance of the pipe. The resulting two-fluid model that includes Eqs. (5), (6-a), (7) and (8-b) is called free pressure model. The form of free pressure model is conservative. Thus, using suitable numerical methods for hyperbolic differential equations is easier.R_k is the volume fraction of phase kth which can be calculated as follows:

$$R_K = \frac{A_K}{A} \tag{9}$$

According to Eq. (9) for calculating the volume fraction, the geometrical constraint relation in Eq. (7) can be rewritten as the following form:

$$R_L + R_G = 1 \tag{10}$$

2.2 Closure Equations

Closure equations that are required to the two-fluid model are comprised of wall-gas phase shear stress, wall-liquid phase shear stress and shear stress at the interface of two phases. The distribution of the shear stress on the pipe wall is very important in determining the turbulence structure inside the pipe as well as the flow resistance (Hua et al. 2012). The following equations are used to calculate wall-gas phase stress, wall-liquid phase stress and interfacial shear stress, respectively (Montini 2011):

$$\tau_G = \frac{1}{2} f_G \rho_G V_G |V_G| \tag{11}$$

$$\tau_L = \frac{1}{2} f_L \rho_L V_L |V_L| \tag{12}$$

$$\tau_I = \frac{1}{2} f_I \rho_G (V_G - V_L)|V_G - V_L| \tag{13}$$

In order to obtain the shear stresses, fanning friction factors (f_G, f_L and f_I) should be calculated. f_G, f_L and f_I represent gas friction factors, liquid friction factors and interface friction factors, respectively. To calculate the friction factors of gas and liquid phases, the existing equations for single-phase flows are usually used, in which a suitable hydraulic diameter is applied for each fluid instead of inner diameter.

$$D_{hG} = \frac{4A_G}{S_G + S_L} \tag{14}$$

$$D_{hL} = \frac{4A_L}{S_L} \tag{15}$$

$$Re_G = \frac{\rho_G D_{hG} |V_G|}{\mu_G} \tag{16}$$

$$Re_L = \frac{\rho_L D_{hL} |V_L|}{\mu_L} \tag{17}$$

In the above equations, D_{hk} and Re_k represent the hydraulic diameter and Reynolds number of kth phase, respectively. μ_k is dynamic viscosity of kth phase. The properties of the fluids are shown below:

- Liquid phase dynamic viscosity: 1.003×10^{-3} kg/m · s
- Gas phase dynamic viscosity: 1.7894×10^{-5} kg/m · s

Required equations to calculate the wet environment of phases (Conte et al. 2014) in Fig. 1 are:

$$S_L = D\left(\frac{\emptyset}{2}\right) \tag{18}$$

$$S_G = D\left(\pi - \frac{\emptyset}{2}\right) \tag{19}$$

$$S_I = D * \sin\left(\frac{\emptyset}{2}\right) \tag{20}$$

$$\frac{dA_L}{dh_L} = D \sin\left(\frac{\emptyset}{2}\right) \tag{21}$$

$$A_L = \frac{D^2}{8}(\emptyset - \sin\emptyset) \tag{22}$$

$$h_L = \frac{D}{2}\left(1 - \cos\frac{\emptyset}{2}\right) \tag{23}$$

$$\emptyset = \pi R_L + \left(\frac{3\pi}{2}\right)^{\frac{1}{3}}\left(1 - 2R_L + R_L^{\frac{1}{3}} - R_G^{\frac{1}{3}}\right) \tag{24}$$

where $\emptyset$ is the stratification angle (Fig. 1).

The pipe surface is considered rough and average surface roughness is assumed equal to $\varepsilon = 4.61 \times 10^{-5}$ (Ansari and Shokri 2011). Friction factor of gas-phase wall is calculated using the following equation (Omgba-Essama 2004):

$$f_G = \max\left[\frac{16}{Re_G}, 0.001375\left[1 + \left[2 \times 10^4 \left(\frac{\varepsilon}{D_{hG}}\right) + \frac{10^6}{Re_G}\right]^{\frac{1}{3}}\right]\right] \tag{25}$$

Friction factor of liquid-phase wall is obtained as follows, using the max method (Omgba-Essama 2004):

$$\begin{cases} f_L = \max\left[\frac{24}{Re_L}, \frac{0.263}{R_L}\sqrt{\frac{D_{hL}}{Re_L D}}\right] & \text{if} \quad j_G > 5 \text{ m/s} \\ f_L = \max\left[\frac{16}{Re_L}, 0.001375\left[1 + \left[2 \times 10^4 \left(\frac{\varepsilon}{D_{hL}}\right) + \frac{10^6}{Re_L}\right]^{\frac{1}{3}}\right]\right] & \text{otherwise} \end{cases} \tag{26}$$

Finally, the friction factor at the interface of two phases is expressed as follows, using the max method (Omgba-Essama 2004):

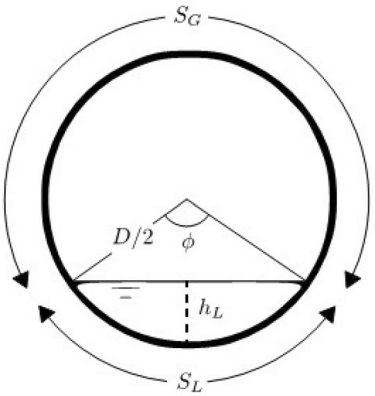

Fig. 1 Pipe cross-sectional area

$$\begin{cases} f_I = f_G & \text{for} \quad j_G < 5 \text{ m/s} \\ f_I = f_G \left\{ 1 + \max \left[0, 15 \left(\frac{j_G}{5} - 1 \right) \sqrt{\frac{h_L}{D}} \right] \right\} & \text{for} \quad j_G \geq 5 \text{ m/s} \end{cases} \tag{27}$$

In Eq. (27), D represents the pipe diameter and j_G is superficial velocity of the gas phase.

2.3 Analysis of Hyperbolic Free-Pressure Two-Fluid Model

Two-phase flow models are very susceptible depending on whether the characteristic values of differential equations are real or complex. If the values are characterized as complex, the model will be an ill-posed condition. The result of such equations is an unlimited instability and will not converge to a unit value. If the characteristic values of differential equations are real, the model is in the well-posed condition and the problem of unlimited instability will be resolved (Ransom and Hicks 1984). The characteristic value of a set of differential equations can be obtained from the hyperbolic analysis.

Hyperbolic analysis of governing equations for the two-fluid model has been proposed by Omgba-Essama (2004) for obtaining the roots of the pressure-free two-fluid model. The two real roots of characteristic equation are as follows:

$$\lambda_{1,2} = \begin{cases} \lambda_1 = \dfrac{(V_L + \chi V_G) - \sqrt{\Delta^S}}{1 + \chi} \\ \lambda_2 = \dfrac{(V_L + \chi V_G) + \sqrt{\Delta^S}}{1 + \chi} \end{cases} \tag{28}$$

In the above equation:

$$\Delta^S = -\chi (V_G - V_L)^2 + (1 + \chi) \frac{\Delta \rho g \cos \beta A_L}{\rho_L A_L'} \tag{29}$$

$$\chi = \frac{\rho_G R_L}{\rho_L R_G} \tag{30}$$

where

$$A_L' = \frac{dA_L}{dh_L} \tag{31}$$

It is clear that the eigenvalues are only real when $\Delta^S \geq 0$. In fact, the range in which the roots of the characteristic equation are real is the well-posedness range of the model (Omgba-Essama 2004). For pressure-free models, this range can be obtained from the following equation:

$$(V_G - V_L)^2 \leq \frac{\Delta \rho (\rho_L R_G + \rho_G R_L)}{\rho_G R_L \rho_L} g \cos \beta \frac{A_L}{A_L'} \tag{32}$$

Equation (32) is known as the principle of inviscid Kelvin–Helmholtz (IKH). If the velocity difference between the two phases exceeds this value, the pressure-free model becomes ill-posed (Ansari and Shokri 2011). This is a major limitation of pressure-free model.

3 Numerical Solution of Equations

3.1 Numerical Methods

Equations (5) and (6-a) can be written in compact conservative which makes them suitable for numerical solution as:

$$\frac{\partial Q}{\partial t} + \frac{\partial F}{\partial x} = H \tag{33}$$

The above equation is an overview of a conservative hyperbolic system of partial differential equations, where Q is the representative vector of conservative variables (e.g., mass or momentum). Vectors F and H are the algebraic functions of conservative variables and are known as flux and source terms, respectively.

In the present research, the solution method is a clear finite-difference method where its discretized form is as follows:

$$Q_i^{n+1} = Q_i^n + \frac{\Delta t}{\Delta x} \left(\hat{F}_{i-1/2} - \hat{F}_{i+1/2} \right) + \Delta t H_i \tag{34}$$

In Eq. (34), Δt represents time step, Δx represents spatial step size, superscript n and $n + 1$ represent the current and the previous time step, respectively. Q is the representative of solver vector; $\hat{F}$ and H indicate numerical flux and the source term.

Selection of the appropriate numerical solution method for the chosen mathematical model is very important. Four following numerical methods will be studied in this research.

3.1.1 Lax–Friedrichs Numerical Method

This method is an explicit first-order approach in terms of space and time (Hirsch 1990). Flux term is calculated as follows:

$$\hat{F}_{i+1/2}^{LF} = \frac{1}{2} \left(F_{i+1}^n + F_i^n \right) - \frac{\Delta x}{2 \Delta t} \left(Q_{i+1}^n - Q_i^n \right), \tag{35}$$

where the numerical flux value at mesh point i is defined by $F_i^n = F\left(Q_i^n\right)$ with the function F representing the physical expression of the flux terms described by the mathematical model under investigation.

3.1.2 Rusanov Numerical Method

This method is an explicit first-order approach which uses the maximum value of characteristic model by hyperbolic

analysis (Omgba-Essama 2004). Flux term here is calculated as follows:

$$\hat{F}^{\mathrm{Rus}}_{i+1/2} = \frac{1}{2}\left(F\left(Q^n_i\right) + F\left(Q^n_{i+1}\right) - \lambda_{i+1/2}\left(Q^n_{i+1} - Q^n_i\right)\right) \tag{36}$$

$$\lambda_{i+1/2} = \max\left(\max\left|\lambda^k_i\right|,\ \max\left|\lambda^k_{i+1}\right|\right) \quad k = 1, N_{\mathrm{eq}} \tag{37}$$

where N_{eq} is the number of equations of system and $\lambda_{i+1/2}$ is the average wave velocity.

3.1.3 Richtmyer Numerical Method

The method is an explicit numerical model. From the time and space viewpoint, it is a second-order method consisting of two steps (Hirsch 1990). Flux expression can be calculated as the following form:

$$Q^n_{i+1/2} = \frac{1}{2}\left(Q^n_i + Q^n_{i+1}\right) \tag{38}$$

$$Q^{n+1/2}_{i+1/2} = Q^n_{i+1/2} - \frac{\Delta t}{2\Delta x}\left(F^n_i - F^n_{i+1}\right) + \frac{\Delta t}{2}H\left(Q^n_{i+1/2}\right) \tag{39}$$

$$\hat{F}^{RI}_{i+1/2} = F\left(Q^{n+1/2}_{i+1/2}\right) \tag{40}$$

3.1.4 FCT Numerical Method

FCT is the first high-precision method by Boric and Book (1973). This method is a predictor/corrector approach in which a part of diffusion enters the system in the prediction stage where the other parts leave the system in anti-diffusion stage in order to eliminate the extreme points in the flow field. FCT is composed of five stages and explained in the following form (Boris and Book 1973). Q^n is the solution at the previous time step, and $\tilde{Q}$ is the new answer which has been obtained via Richtmyer second-order scheme.

1–Generation of diffusive fluxes

$$F^d_{i+1/2} = \upsilon_{i+1/2}\left(Q^n_{i+1} - Q^n_i\right) \tag{41}$$

2–Diffusion of the solution

$$Q^d_i = \tilde{Q}_i + \left(F^d_{i+1/2} - F^d_{i-1/2}\right) \tag{42}$$

3–Generation of anti-diffusive fluxes

$$F^{\mathrm{ad}}_{i+1/2} = \gamma_{i+1/2}\left(\tilde{Q}_{i+1} - \tilde{Q}_i\right) \tag{43}$$

4–Limitation of the anti-diffusive fluxes

$$F^{\mathrm{cad}}_{i+1/2} = s \cdot \max\Big(0,\ \max\Big(s \cdot \left(\tilde{Q}_{i+1} - Q^d_i\right), \left|F^{\mathrm{ad}}_{i+\frac{1}{2}}\right|, s \cdot \left(\tilde{Q}_{i+2} - Q^d_{i+1}\right)\Big)\Big) \tag{44}$$

$$s = \mathrm{sign}\left(F^{\mathrm{ad}}_{i+1/2}\right) \tag{45}$$

5–Generation of inter-cell flux

$$\hat{F}^{\mathrm{FCT}}_{i+1/2} = F^{\mathrm{cad}}_{i+1/2} - F^d_{i+1/2} \tag{46}$$

For the present numerical scheme, the diffusion and anti-diffusion coefficients, i.e., υ and γ are obtained as follows (Hoffmann and Chiang 2000):

$$\upsilon = \frac{1}{6}\left(1 + 2(CFL)^2\right) \tag{47}$$

$$\gamma = \frac{1}{2}\left(1 + (CFL)^2\right) \tag{48}$$

CFL is the Courant Friedrichs Levy Number.

3.2 Determination of Time Step

In the present research, for the numerical solution of the governing equations, spatial step size, i.e., Δx, will be determined first. Since the employed numerical methods are categorized as explicit approaches, they have stability condition. The stability of this approach is Courant Friedrichs Levy Number $(CFL) \leq 1$. Given Δx and *CFL* values, time step is calculated as follows:

$$\Delta t = CFL\frac{\Delta x}{\lambda^n_{\max}} \tag{49}$$

$\lambda^n_{\max}$ is the maximum value of wave velocity in the flow field at the previous time step. $\lambda^n_{\max}$ is selected at each time step, and concerning the variability of $\lambda^n_{\max}$, the solution method has a variable time step.

$$\lambda^n_{\max} = \max_j\left\{\max_k\left|\lambda^k_j\right|\right\} \quad \text{for} \quad j = 1, \ldots, M \quad k = 1, N_{\mathrm{eq}}, \tag{50}$$

where N_{eq} is the number of equations of the system and also λ^k_j is wave velocity in each computational cell.

3.3 Boundary Conditions

For a computing domain (0, *L*) discretized into *M* computing cells of length Δx, we require special conditions at the boundary positions $x = 0$ and $x = \mathrm{L}$ as illustrated in Fig. 2. These boundary conditions are expected to provide for test

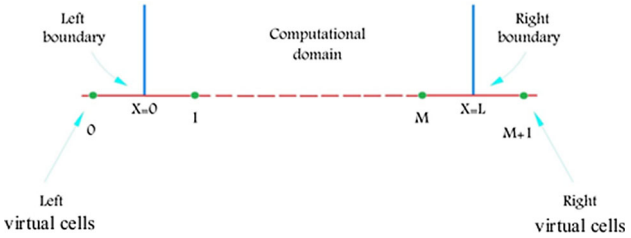

Fig. 2 Computing field and virtual cells

case the numerical fluxes $\hat{F}_{1/2}$ and $\hat{F}_{M+1/2}$, which are required by finite-difference discretization such as Eq. (34) in order to advance the extreme cells 1 and M to the next time level. For this, in the input and output, virtual grid will be considered and zeroth-order extrapolation for the virtual points will be used for the flux in entry and outlet.

4 Slug Flow Modeling

4.1 Simulation of Slug Flow Initiation

Gas and liquid phases are considered air with a density of 1.14 kg/m^3 and water with a density of 1000 kg/m^3, respectively. A horizontal pipe with the length of 5 m and the diameter of 0.078 m is selected, in which two phases flow in stratified and stable types initially. The inlet superficial gas velocity is equal to 6.532 m/s, and inlet superficial liquid velocity is equal to 0.532 m/s. When the slug is formed, the volume fraction of the liquid phase has reached one where the volume fraction of gas phase has tended to zero. Since the volume fraction of the gas phase is multiplied on both sides of the gas momentum equation, this equation becomes singular. In order to avoid wrong value velocities for the gas phase resulting from solving singular gas momentum equation in an area which only includes liquid phase, the gas phase equation is eliminated in this area and gas velocity is considered zero. In other areas, the two-fluid model equation is solved completely.

After the unknown variables are obtained, they should satisfy Eq. (32) in order to ensure the reality of the roots of the trail equation. Otherwise, the roots of the trail equation are imaginary and the calculation will be stopped.

As seen from Fig. 3, the initial condition considered in slug flow regime is movable. In other words, the initial conditions are located on the unstable inviscid Kelvin–Helmholtz line and are in transition from stratified pattern to slug pattern.

The inviscid Kelvin–Helmholtz instability line is known as the well-posed region of two-fluid model (Louaked et al. 2003).

4.2 Boundary Conditions and Initial Conditions

The value of volume fraction of the liquid phase at the initial moment is 0.526. The values of initial velocity of each phase through the pipe are obtained using volume fraction and superficial velocity of each phase at inlet pipe. The boundary conditions are considered equal to the initial conditions at entrance. Also, for outlet pipe boundary conditions, a fully developed condition is considered.

5 Result and Discussion

Figures 4, 5, 6 and 7 show the initiation point of the slug flow map for different computational cells, using four different numerical methods, Lax-Friedrichs, Rusanov,

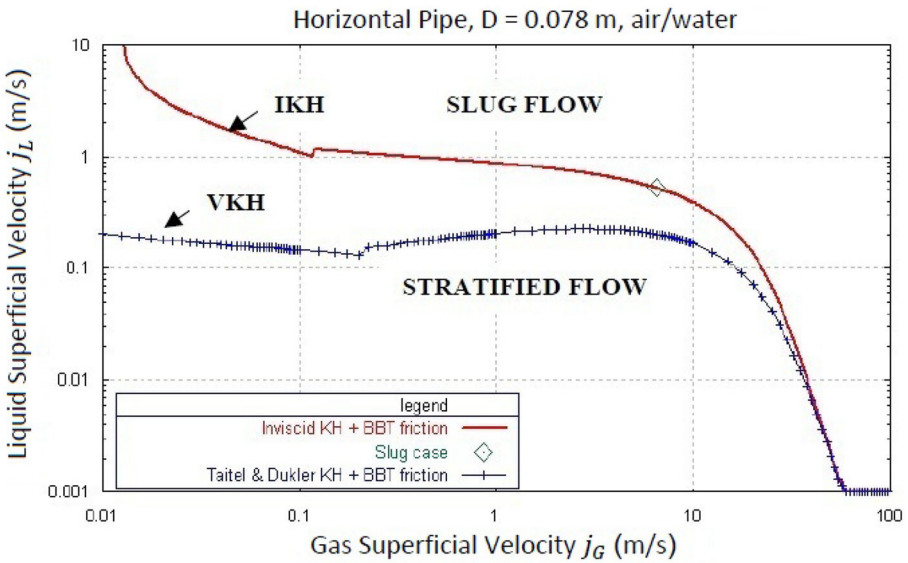

Fig. 3 Inviscid Kelvin–Helmholtz (IKH) transition lines from stratified flow

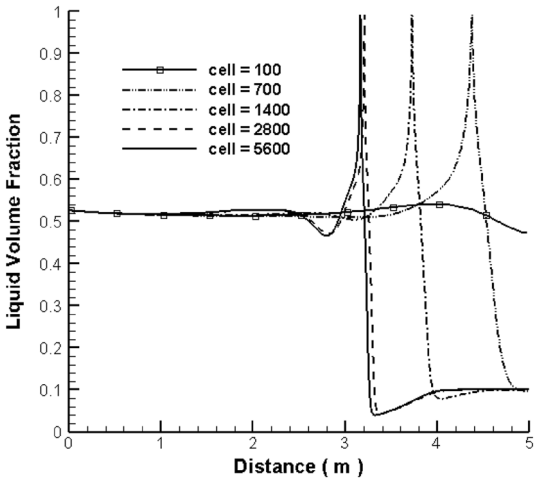

Fig. 4 Initiation point of the slug flow map for different computational cells using Lax–Friedrichs numerical method

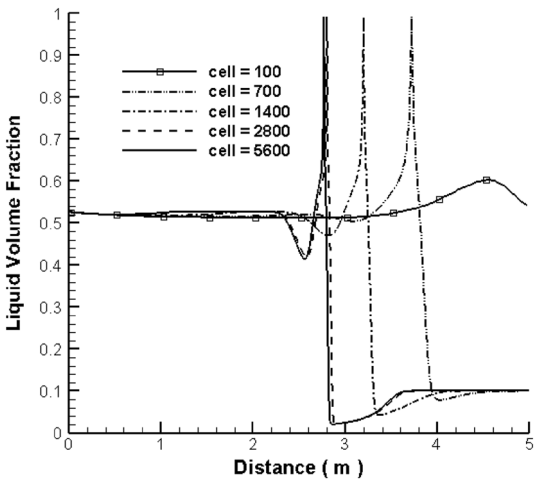

Fig. 5 Initiation point of the slug flow map for different computational cells using Rusanov numerical method

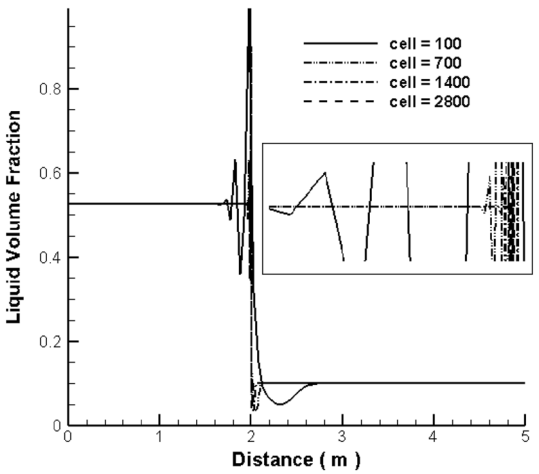

Fig. 6 Initiation point of the slug flow map for different computational cells using Richtmyer numerical method

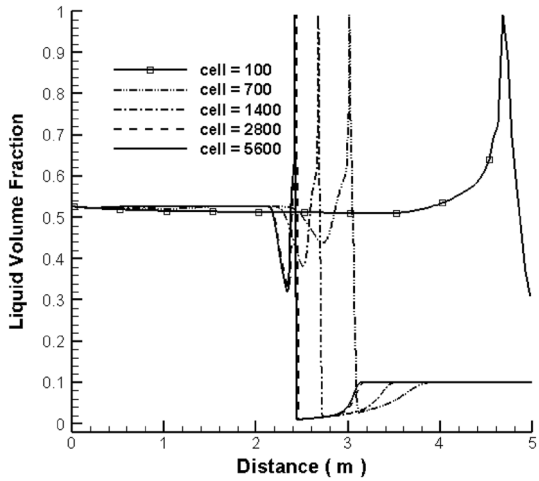

Fig. 7 Initiation point of the slug flow map for different computational cells using FCT numerical method

Richtmyer, and FCT, respectively. Computational time and Courant–Friedrichs–Lewy number (*CFL*) are considered 3 s and 0.3, respectively.

Figures 4, 5 and 7 show the slug flow initiation point for different computational cells 100, 700, 1400, 2800 and 5600 using Lax-Friedrichs method, Rusanov method and FCT method. Results indicated that with 2800 computational cells, solutions are independent of the computational cell for those three methods. Thus, this computational cell is used for the analysis of the following results. Figure 6 shows the slug flow initiation point for 100, 700, 1400 and 2800 computational cells based on the Richtmyer numerical method. Results show that the Richtmyer numerical method has an oscillatory nature where, reducing the size of the computational cell the oscillations become greater. As a result, the Richtmyer numerical method is not suitable for modeling the slug flow regime. Richtmyer numerical method is a second-order method which has third-order error. This type of error leads to numerical dispersion for solutions near the discontinuity due to the formation of slug flow regime.

Figure 8 shows the accuracy of different methods for predicting the slug flow initiation point. The calculations are based on 2800 computational cells. Time of calculation and Courant–Friedrichs–Lewy number are 3 s and 0.3, respectively. The results are compared with those achieved by Ansari (1998) experimentally to validate the computer program in Fig. 9.

In Fig. 9 it is indicated that no considerable difference exists between the points of slug flow initiation for 2800 and 5600 computational cells for Lax-Friedrichs, Rusanov and FCT numerical methods. Therefore, in the 2800 cells, we have gird independence results.

In Figs. 4 and 5, the slug flow regime initiation for the various computational cells is indicated for Lax-Friedrichs

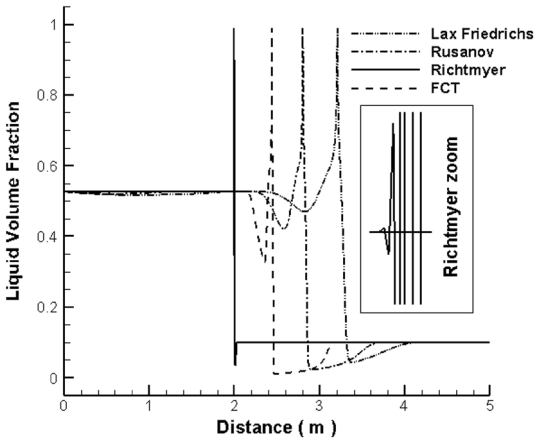

Fig. 8 Comparison of various numerical accuracies in predicting the beginnings of slug flow regime

numerical method and Rusanov numerical method. The results also show that for 100 computational cells for Lax-Friedrichs numerical method and Rusanov numerical method, the slug flow regime is not formed. Therefore, for the validation of numerical results, the 100 computational cells are not used for these two methods.

Figure 9 shows that the Lax-Friedrichs numerical method has the lowest accuracy in prediction of the slug flow regime initiation when compared to the experimental results, whereas the FCT method is the most accurate method for the prediction of slug flow regime initiation. Also, it can be seen that the prediction of slug flow regime initiation by Lax-Friedrichs numerical method has a large deviation compared to the experimental results. The first-order Lax-Friedrichs predicts the discontinuities resulted from the formation of the slug flow which are with numerical dispersion in the flow field. Lax-Friedrichs method is a first-order method with the second-order error.

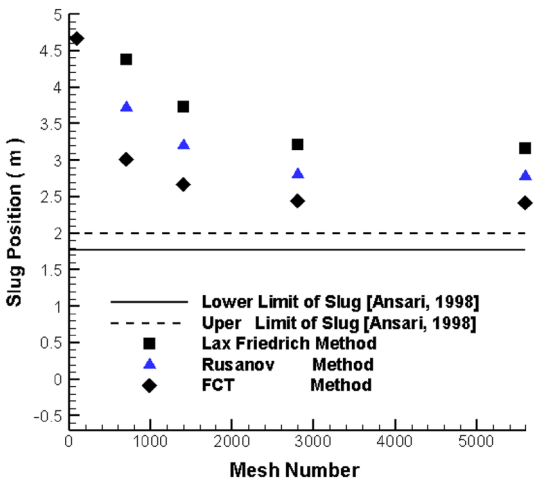

Fig. 9 Comparison of obtained initiation point of slug flow with experimental results

The second-order error causes a numerical diffusion which leads to a discontinuity dispersion in the solution field. Thus, Lax-Friedrichs numerical method cannot predict the slug flow initiation with high accuracy.

It also can be seen that the Rusanov numerical method predicts the slug flow initiation more accurately compared to the Lax-Friedrichs numerical method (Fig. 9). Rusanov numerical method also is a first-order method having second-order error. Second-order error is a numerical diffusion leading to the dispersion of discontinuity in the flow field. As far as Rusanov numerical method is a characteristics-based method which owns more accurate information about the flow characteristics, thus, Rusanov numerical method generates less numerical diffusion in comparison with the Lax-Friedrichs and therefore can predict the slug flow initiation with high accuracy.

Richtmyer numerical method is a second-order method having third-order error. This type of error causes the solutions to be dispersed in the flow field. Thus, this method cannot be an appropriate method for prediction of the slug flow initiation. As it is observed in the accuracy verification diagram of the numerical methods for the prediction of the slug flow initiation, the Richtmyer numerical scheme is not utilized.

From the slug flow initiation point obtained via FCT method which is shown in Fig. 9, it is indicated that FCT method predicts the slug flow initiation point more accurately compared to the Lax-Friedrichs and Rusanov numerical methods.

In FCT method, the output of numerical solution is obtained via Richtmyer numerical method which is a second-order method and for the flux correction, artificial diffusion is incorporated. The artificial diffusion is incorporated into the FCT method for flux correction because of the numerical dispersion that exists in the second-order methods, and according to the FCT method, this numerical dispersion has disappeared. FCT method is the most accurate scheme in the prediction of the slug flow initiation among the methods introduced in this paper.

In Figs. 10 and 11, the time history of interfacial waves that is converted to slug flow is given. The growth of interfacial waves in 0.3 and 0.4 s for all Lax-Friedrichs, Rusanov, and FCT numerical methods is indicated. The computational cell and Courant–Friedrichs–Lewy number are considered as 2800 and 0.3, respectively.

As it is indicated in Figs. 10 and 11, the prediction of volume fraction of liquid-phase FCT method in various time histories is greater than Rusanov and Lax-Friedrichs numerical methods. In fact, the interfacial waves grow with the time. In Lax-Friedrichs numerical method, great numerical diffusion exists in the flow field compared to Rusanov numerical method. In 0.3 s, the waves have not grown and in 0.4 s the waves start to grow, regarding the

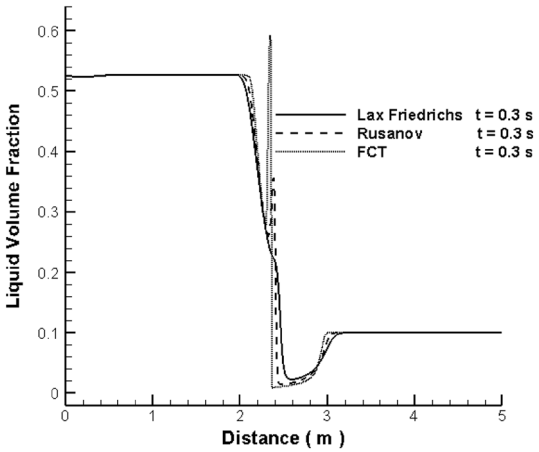

Fig. 10 Time history of the growth of interfacial waves in 0.3 s

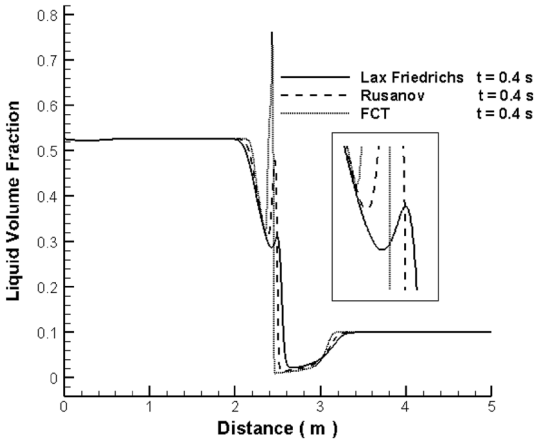

Fig. 11 Time history of the growth of interfacial waves in 0.4 s

Lax-Friedrichs method. As a result, the amount of wave growth in Lax-Friedrich numerical method is obviously lower than the two other numerical schemes.

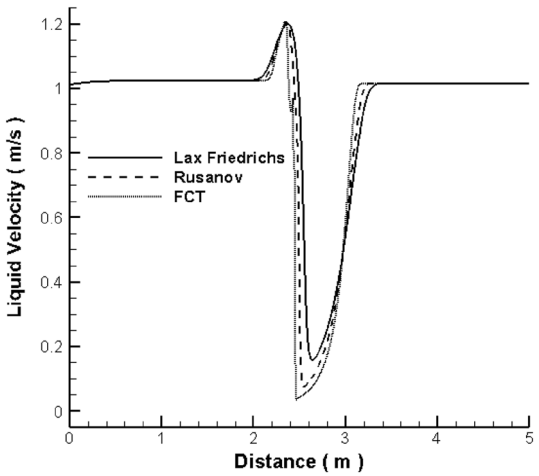

Fig. 12 Comparison of the liquid phase velocity profile changes for different numerical schemes in 0.4 s

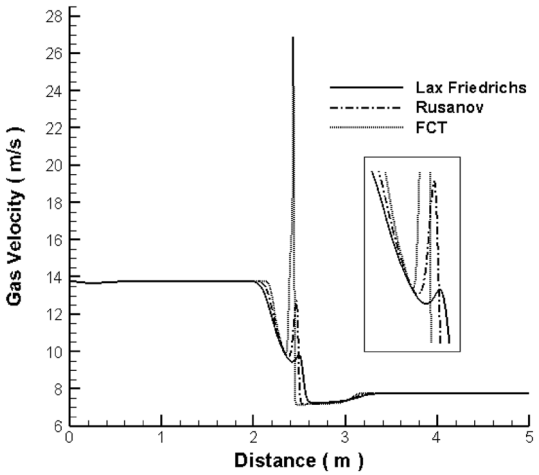

Fig. 13 Comparison of the gas phase velocity profile changes for different numerical schemes in 0.4 s

Figures 12 and 13 present the variation of the liquid- and gas-phase velocity profile for different numerical methods. The number of computational cells and Courant–Friedrichs–Lewy number are 2800 and 0.4 s, respectively.

As the growth of volume fraction of liquid phase increases, the gas flow cross section decreases and the liquid flow cross section increases. Therefore, the velocity of the liquid and the gas phase decreases and increases, respectively. According to Fig. 11, the volume fraction of the liquid phase of FCT method is the highest compared to the other methods. As a result, the liquid phase velocity reduces sharply as shown in Fig. 12, and the gas velocity increases remarkably as plotted in Fig. 13.

6 Conclusion

This paper employed Rusanov, Richeymer and FCT numerical methods to model the slug flow initiation point and its growth in horizontal pipes. Among these three methods, FCT method is the most accurate scheme in predicting the slug flow initiation point. Lax-Friedrichs numerical method due to the high numerical dispersion in the flow field has the least accuracy in the prediction of slug flow initiation. Rusanov numerical method such as Lax-Friedrichs numerical method is classified as a first-order method having a second-order error. Concerning that Rusanov numerical method is a flow characteristic-based method, more accurate information can be obtained from flow characteristics. So, this method has lower numerical dispersion compared to the Lax-Friedrichs scheme, and hence it can predict the slug flow initiation point with higher accuracy in comparison with the Lax-Friedrichs scheme. Due to the oscillatory nature of the Richtmyer numerical method in the discontinuity region caused by the

slug flow formation, it is not an appropriate method for modeling the slug flow regime.

References

Ansari MR (1998) Dynamical behavior of slug initiation generated by short waves in two-phase air-water stratified flow. ASME Heat Transf Div Publ HTD 361:289–296

Ansari M, Shokri V (2011) Numerical modeling of slug flow initiation in a horizontal channels using a two-fluid model. Int J Heat Fluid Flow 32(1):145–155

Bonizzi M, Issa R (2003a) A model for simulating gas bubble entrainment in two-phase horizontal slug flow. Int J Multiph Flow 29(11):1685–1717

Bonizzi M, Issa R (2003b) On the simulation of three-phase slug flow in nearly horizontal pipes using the multi-fluid model. Int J Multiph Flow 29(11):1719–1747

Bonzanini A, Picchi D, Poesio P (2017) Simplified 1D incompressible two-fluid model with artificial diffusion for slug flow capturing in horizontal and nearly horizontal pipes. Energies 10(9):1372

Boris JP, Book DL (1973) Flux-corrected transport. I. SHASTA, a fluid transport algorithm that works. J Comput Phys 11(1):38–69

Carneiro J, Ortega A, Nieckele A (2005) Influence of the interfacial pressure jump condition on the simulation of horizontal two-phase slug flows using the two-fluid model. WIT Trans Eng Sci 50(3):123–132

Cazarez-Candia O, Benitez-Centeno O, Espinosa-Paredes G (2011) Two-fluid model for transient analysis of slug flow in oil wells. Int J Heat Fluid Flow 32(3):762–770

Conte MG, Cozin C, Barbuto FA, Morales RE (2014) A two-fluid model for slug flow initiation based on a lagrangian scheme. In: Proceeding of the American society of mechanical engineers, pp V002T20A003–V002T20A003

Hanyang G, Liejin G (2005) Stability of stratified flow and slugging in horizontal gas–liquid flow. Prog Nat Sci 15(11):1026–1034

Hirsch H (1990) Numerical computation of internal and external flows. Comput Methods Inviscid Viscous Flows 2:536–556

Hoffmann KA, Chiang ST (2000) Computational fluid dynamics volume I. In: Engineering education system, Wichita, Kan, USA

Hua J, Langsholt M, Lawrence C (2012) Numerical simulation of single elongated bubble propagation in inclined pipes. Progr Comput Fluid Dyn, Int J 12(2–3):131–139

Ishii M (1975) Thermo-fluid dynamic theory of two-phase flow. Eyrolles, Paris

Ishii M, Mishima K (1984) Two-fluid model and hydrodynamic constitutive relations. Nucl Eng Des 82(2):107–126

Issa R, Kempf M (2003) Simulation of slug flow in horizontal and nearly horizontal pipes with the two-fluid model. Int J Multiph Flow 29(1):69–95

Issa R, Bonizzi M, Barbeau S (2006) Improved closure models for gas entrainment and interfacial shear for slug flow modelling in horizontal pipes. Int J Multiph Flow 32(10):1287–1293

Issa R, Castagna J, Sheikh A (2011) Accurate simulation of intermittent/slug flow in oil and gas pipelines. In: 15th international conditioning on multiphase production technology, Cannes, France, June 15–17

Louaked M, Hanich L, Thompson C (2003) Well-posedness of incompressible models of two-and three-phase flow. IMA J Appl Math 68(6):595–620

Montini M (2011) Closure relations of the one-dimensional two-fluid model for the simulation of slug flows. PhD Thesis, Imperial College London, London

Omgba-Essama C (2004) Numerical modelling of transient gas–liquid flows (application to stratified & slug flow regimes). PhD Thesis, Cranfield University

Ransom VH, Hicks DL (1984) Hyperbolic two-pressure models for two-phase flow. J Comput Phys 53(1):124–151

Shokri V, Esmaeili K (2017) Comparison of the effect of hydrodynamic and hydrostatic models for pressure correction term in two-fluid model in gas–liquid two-phase flow modeling. J Mol Liq 237:334–346

Simões EF, Carneiro JN, Nieckele AO (2014) Numerical prediction of non-boiling heat transfer in horizontal stratified and slug flow by the Two-Fluid Model. Int J Heat Fluid Flow 47:135–145

Ujang PM, Lawrence CJ, Hale CP, Hewitt GF (2006) Slug initiation and evolution in two-phase horizontal flow. Int J Multiph Flow 32(5):527–552

Wallis GB (1969) One-dimensional two-phase flow. McGraw-Hill Companies, New York

Wang X, Guo L, Zhang X (2007) An experimental study of the statistical parameters of gas–liquid two-phase slug flow in horizontal pipeline. Int J Heat Mass Transf 50(11):2439–2443

Watson M (1990) Non-linear waves in pipeline two-phase flows. In: Third international conference on hyperbolic problems

Woodburn P, Issa R (1998) Well-posedness of one-dimensional transient, two-fluid models of two-phase flows. In: Third international conditioning of multiphase flow, Lyon, France, June 8–12

Zeng Q, Aydemir N, Lien F, Xu T (2015) Comparison of implicit and explicit AUSM-family schemes for compressible multiphase flows. Int J Numer Meth Fluids 77(1):43–61